RESEARCH ARTICLE

Experimental study on static and dynamic mechanical properties of phosphogypsum

Ting Lu [1,2] · Wensong Wang [1,2] · Zuoan Wei [1,2] · Yonghao Yang [1,3] · Guansen Cao [1,2]

Abstract

Phosphogypsum (PG) is a solid waste product of the wet-process phosphoric acid industry that accumulates in large amounts on the ground, forming PG ponds. In recent years, the amount of PG produced and discharged into ponds has increased significantly with the increase in the market demand for phosphate fertilizers. To enrich the basic knowledge of PG properties and provide basic data for the stability analysis of PG dams, a series of laboratory geotechnical tests, including permeability tests, compressibility tests, triaxial shear tests, and dynamic triaxial tests, were conducted in this study. During the preparation of the test samples, solubility and high-temperature dehydration of PG were considered. The results indicated that PG exhibits medium compressibility and medium to weak permeability characteristics. The stress-strain curves of the triaxial shear tests were divided into three typical stages: initial deformation stage, strain hardening stage, and destruction stage. With increasing dry density and consolidation confining pressure, both the shear strength and deformation modulus significantly increased. The relationship between the deformation modulus and confining pressure gradually changed from linear to logarithmic with increasing density. The liquefaction resistance curves (CSR–N_L curves) of PG were expressed by power functions. With increasing dry density, the curves shifted higher and became steeper. Compared with the Hardin–Drnevich model, the Davidenkov model was found to be more suitable for describing the relationship between the dynamic shear modulus ratio and damping ratio of PG and the dynamic shear strain. Furthermore, compared with those of tailings and natural soils, the engineering mechanical properties of PG were relatively poor, which may be related to its uniform particle distribution and neat particle stacking structure.

Keywords Waste management · Geotechnical test · Shear strength · Liquefaction · Dynamic shear modulus · Damping ratio

Introduction

Phosphogypsum (PG) is a solid waste product of the wet-process phosphoric acid industry, and approximately 4–6 t of PG is produced for every ton of phosphoric acid (Rashad

2017). The physical and chemical properties of PG are similar to those of conventional gypsum because the main phase composition of PG is also dihydrated calcium sulfate ($CaSO_4 \cdot 2H_2O$) (Canut et al. 2008). Therefore, PG has been utilized in many fields, in construction materials (Tian et al. 2016), agricultural fertilizers (Kammoun et al. 2017), production materials (Cuadri et al. 2014; Ma et al. 2018), underground filling materials (Chen et al. 2017; Min et al. 2019), subgrade backfill materials (Li et al. 2020), and the recycling of rare earth elements (Hammas-Nasri et al. 2019; Rychkov et al. 2018). Among them, the application in cement has presented good results. PG can be used as a cement retarder (Shen et al. 2012), used to prepare calcium sulfoaluminate cement (Wu et al. 2020), and used as an additive to improve the mechanical properties of cement-stabilized soil (Zeng et al. 2020). However, PG contains many impurities, such as water-soluble phosphate, water-soluble fluoride, and P_2O_5 substituted in the gypsum crystal lattice (Jalali et al. 2019). Currently, only 15% of the annual worldwide production of PG is reused

Responsible Editor: Ta Yeong Wu

✉ Wensong Wang
   wws@cqu.edu.cn

✉ Zuoan Wei
   weiza@cqu.edu.cn

1   State Key Laboratory of Coal Mine Disaster Dynamics and Control, Chongqing University, Chongqing 400044, China

2   School of Resources and Safety Engineering, Chongqing University, Chongqing 400044, China

3   School of Civil Engineering, Chongqing Jiaotong University, Chongqing 400074, China

or recycled (Geraldo et al. 2020). A considerable amount of unused PG has been piled onto the ground, forming many PG ponds, which is a type of tailing pond and can be categorized into wet ponds and dry ponds.

A tailing pond has a high potential for debris flow. Failure of a tailing dam leads to disastrous consequences, causing considerable loss of life and property and serious environmental pollution. In recent years, tailing dam failure accidents have occurred in Brazil (Escobar 2015; Hudson-Edwards 2016), Japan (Ishihara et al. 2015), China, and other countries (Wei et al. 2013). PG ponds are necessary production facilities for phosphate mines and phosphorus chemical companies, but they are also among the most significant sources of danger. The massive accumulation of PG brings many problems in terms of safety risks and environmental problems.

In recent years, as the market demand for phosphate fertilizers has increased, the amount of PG produced and discharged into PG ponds has increased correspondingly. The safety concerns of PG ponds have become more severe, and the stability of PG dams is of great concern. Production safety accidents at PG ponds in China have occurred sporadically, causing great loss of life and property. For example, on August 11, 2016, the Longjing Bay PG pond of Guizhou Kailin (Group) Co., Ltd., partially collapsed, resulting in two deaths and one missing person (People's government of Guizhou province 2016). To effectively prevent production safety accidents at PG ponds, the former State Administration of Work Safety of China (now merged into the Ministry of Emergency Management of China) issued the "Notice on Strengthening the Safety Production of Phosphogypsum Pond" in 2017 (Ministry of Emergency Management of the People's Republic of China 2017), and the "Safety Technical Regulations on Phosphogypsum Stack (AQ 2059-2016)" was implemented on March 1, 2017 (State Administration of Work Safety of the People's Republic of China 2016). Wang et al. (2011) conducted a safety assessment on a new PG pond, without performing a detailed analysis of the stability of the PG tailing dam or comprehensively research the mechanical properties of the PG. In general, more studies have focused on environmental problems with PG ponds. However, from a safety perspective, it is imperative to calculate and analyze the stability of PG dams. The mechanical properties of PG provide basic information for stability analysis. More importantly, PG is a special type of tailings that is distinguished from natural soil and conventional tailings in terms of formation, particle geometry, and particle size distribution (Yang et al. 2019). The mechanical properties of PG are distinctive. However, researchers have been mainly concerned with the physical and chemical properties of PG, such as solubility and radioactivity. Therefore, systematic research on the mechanical properties of PG is still limited. Zhang et al. (2007) investigated the relationship between PG moisture content and drying temperature and drying time and the relationship between PG solubility and temperature. They found that PG has obvious dilatancy characteristics under triaxial compression. The investigation of a PG pond by Mi et al. (2015) showed that PG has a high compressibility, internal friction angle, and liquefaction resistance, and its crystal structure can be destroyed during loading. However, their studies did not consider the solubility and dehydration of PG during sample preparation. Therefore, current research on the mechanical properties of PG is very rare and unsystematic.

In this study, a large number of laboratory geotechnical tests (including permeability tests, consolidation tests, triaxial compression tests, and dynamic triaxial tests) are carried out to thoroughly investigate the mechanical properties of PG. In the sample preparation process, the unique properties of PG, which are different from those of general soil, such as dehydration at a high temperature and solubility, were considered. The results provide basic data for the static and dynamic stability analyses of PG dams, thus enriching the basic knowledge of PG mechanics and helping enterprises safely manage PG ponds.

Materials and methods

Materials

The test PG samples were acquired from the Sinochem Fuling Chongqing Chemical Industry Co., Ltd.; this PG was a waste product of the phosphoric acid production performed by the company. PG is dark gray in its natural state and grayish after drying. Its chemical composition is presented in Table 1, and its main physical parameters are summarized in Table 2. The particle size distribution curve of PG is shown in Fig. 1. Tayibi et al. (2009) obtained the micrograph of PG by scanning electron microscopy (SEM). The micrograph depicts that PG has a uniform and prismatic stacking arrangement and a well-defined crystal structure, mostly composed of diamond-shaped and orthogonal crystals.

Sample preparation

The samples were remolded by disturbed PG. Their dry density was determined in accordance with the deposition law and density distribution state of the PG in the pond. In this study, samples with three densities were tested: L1 (ρ_d = 1.200

Table 1 Chemical composition of phosphogypsum (%)

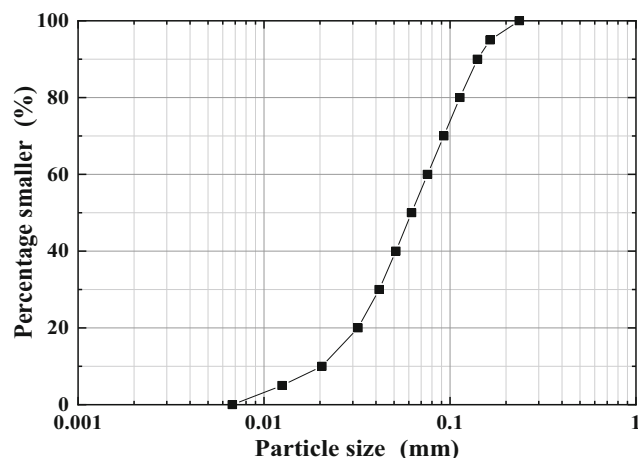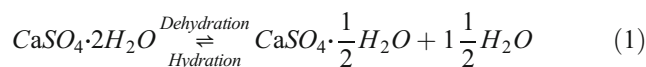| Crystal water	SO$_3$	CaO	P$_2$O$_5$	MgO	Al$_2$O$_3$	Fe$_2$O$_3$	Others
18.45	43.08	29.71	0.71	0.46	0.73	0.30	6.56

Table 2 Physical properties of phosphogypsum

Specific gravity	Liquid limit (%)	Plastic limit (%)	Plastic index	D_{50} (mm)	C_u	C_c
2.37	29.6	17.8	11.8	0.062	3.7	1.1

Note: D_{50} refers to the average particle size, C_u refers to the non-uniform coefficient, and C_c refers to the curvature coefficient

g/cm^3, e = 0.975), L2 (ρ_d = 1.275 g/cm^3, e = 0.859), and L3 (ρ_d = 1.350 g/cm^3, e = 0.756).

The main phase composition of PG is dihydrated calcium sulfate ($CaSO_4·2H_2O$), which contains two crystal waters. Therefore, PG could be dehydrated under certain conditions and converted into semi hydrated gypsum or anhydrite, which is usually researched through calcination tests (Geraldo et al. 2020). The calcination and dehydration characteristics of PG have been reported in detail in some literature. The water-soluble impurities in PG and calcination temperature are important factors affecting the process (Gorbovskiy et al. 2018; Bumanis et al. 2018). Dehydrated PG (hemihydrate or anhydrite) will undergo hydration reactions and coagulation upon contact with water (Chen et al. 2019). The reaction process can be represented by Eq. (1). Therefore, in the preparation of test samples, in addition to complying with the geotechnical test technical specification (the specification adopted in this paper is "Standard for geotechnical testing method" (GB/T 50123-2019)), it is also necessary to refer to the specifications of PG. For example, to avoid losing crystal water during the drying process, the China national standard "Phosphogypsum" (GB/T 23456-2018) suggests that the drying temperature of PG is 40 ± 2 °C (State Administration for Market Regulation of the People's Republic of China 2018), not the 105 °C suggested for natural soil and conventional tailings (Ministry of Housing and Urban-Rural Development of the People's Republic of China 2019).

$$CaSO_4·2H_2O \underset{Hydration}{\overset{Dehydration}{\rightleftharpoons}} CaSO_4·\frac{1}{2}H_2O + 1\frac{1}{2}H_2O \qquad (1)$$

The test samples with three densities were remolded using cylindrical molds, and the compaction apparatus is shown in Fig. 2. The remolded PG samples are also shown in Fig. 2, and the preparation obeys the following procedure:

(i) Preparation of the dry PG and PG saturated solution. The PG was placed in an oven at 40 °C to dry; when it was dry, the PG was then broken and sorted with a geotechnical sieve with a pore size of 2 mm. The PG-saturated solution was prepared using distilled water and PG.

(ii) Preparation of wet PG with a moisture content of 15%. A proper amount of PG-saturated solution was mixed with the sieved dry PG and stirred evenly to prepare a wet PG with a moisture content of 15%, that is, the mass of the solution was 15% of the mass of the corresponding dry PG. To ensure that the water content was uniform within the sample, the samples were placed in a sealed bag for 24 h.

(iii) Preparation of PG samples with three densities. According to the required sample density and mold volume, the masses of the well-mixed wet PG were weighed considering the three densities and different molds. Then, the proper weight of wet PG was compacted into the mold using a compaction apparatus to obtain PG samples with three densities.

According to the geotechnical test technical specification and the requirements of the equipment, for the sizes of the samples, the consolidation test sample was 61.8 mm in diameter and 20 mm in height, and the permeability test specimen was 61.8 mm in diameter and 40 mm in height. The samples were remolded using an integral compaction method. A triaxial compression test sample is 39.1 mm in diameter and 80 mm in height, and a dynamic triaxial test sample is 50 mm in diameter and 100 mm in height. The samples were divided into four layers to remold using a layer-by-layer compaction method.

Test program

Laboratory geotechnical tests were performed to investigate the mechanical properties, their variation law, and key

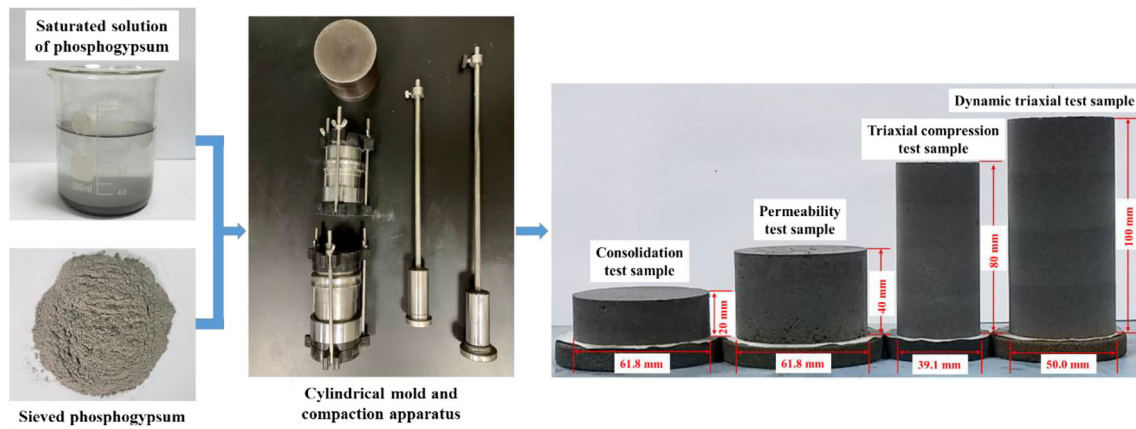**Fig. 1** Particle size distribution of phosphogypsum

Fig. 2 Test samples of phosphogypsum and their preparation process

influential factors of the PG with three dry densities. Four types of tests were selected: permeability tests, consolidation tests, triaxial compression tests, and dynamic triaxial tests.

The laboratory tests were carried out at the State Key Laboratory of Coal Mine Disaster Dynamics and Control at Chongqing University. The testing process and methods are mainly based on the Chinese national standard of the Geotechnical Engineering Test Method (GB/T 50123-2019) (Ministry of Housing and Urban-Rural Development of the People's Republic of China 2019). Given that the results of soil tests, especially triaxial shear tests and dynamic triaxial tests, are sensitive to the saturation degree of the samples, it is necessary to saturate the test samples before carrying out the tests. The saturation process was carried out in accordance with the Chinese Geotechnical Test Method Standard (GB/T 50123-2019) (Ministry of Housing and Urban-Rural Development of the People's Republic of China 2019) and the ASTM standard D4767-11 (ASTM international 2011a). First, CO_2 was pumped into the test samples, and then, the samples were saturated by means of two saturation processes, infiltration saturation and back pressure saturation. Only when the saturation reached 98% or more would the test continue. Moreover, because PG is soluble (Papanicolaou et al. 2009), the PG-saturated solution was used to saturate the samples instead of distilled water, which can avoid unevenness of the samples caused by the dissolution of PG, thereby reducing testing error.

Consolidation tests and permeability tests

The consolidation tests were conducted using a WG-Light-Duty Consolidation Apparatus. The vertical pressures applied during the test ranged from 25 to 3200 kPa, and the duration of each action was 24 h. The permeability tests were conducted using a TST-55 Permeameter. Samples of each dry density were subjected to five tests. Both tests were carried out at a room temperature of 25 ± 1 °C, which was in line with the

relevant rules of ASTM standard D2435/D2435 M-11 (ASTM international 2011b).

Triaxial shear tests

The triaxial shear tests were conducted using a TSZ-6A Strain-controlled Triaxial Test Apparatus (produced by Nanjing Soil Instruments). To obtain the total stress parameter and effective stress parameter of the PG shear strength, triaxial consolidated-undrained (CU) testing at three different confining pressures was carried out, and the confining pressures were set up based on the burial depths in the PG pond. In addition, the ratio of the stress increment to the strain increment is defined as the deformation modulus (E) in this paper. The peak stress was considered the failure indicator of the samples, which was the maximum principal stress difference (deviatoric stress) at the stress-strain curve. The deviatoric stress corresponding to a 15% axial strain (ε) was taken as the peak stress of samples when the stress-strain curve had no peak (Zheng et al. 2019). According to ASTM standard D4767-11, the deviatoric stress in the triaxial test was the measured value minus 1 kPa to consider the influence of the rubber film (ASTM international 2011a).

Dynamic triaxial tests

The dynamic triaxial tests were conducted using a Dynamic Triaxial Testing System (DYNTTS, produced by UK GDS Instruments), which makes it possible to obtain the wave velocity through the bender element test instrument of the system. The consolidation condition in the test is isotropic ($\sigma_1 = \sigma_3$), and samples of each dry density are subjected to tests under three consolidation confining pressures. The dynamic load is a sine wave with a vibration frequency of 1 Hz.

In the liquefaction resistance test, the cyclic load is characterized by the cyclic stress ratio (*CSR*) defined as follows:

$$CSR = \sigma_d/2\sigma_0' \tag{2}$$

$$\sigma_0' = (\sigma_1 + 2\sigma_3)/3 - \mu_0 \tag{3}$$

where σ_d is the amplitude of the dynamic stress, σ_0' is the mean effective confining pressure of the sample, σ_1 and σ_3 are the axial and radial consolidation pressures, and μ_0 is the initial pore water pressure.

The liquefaction resistance of soil is frequently characterized using liquefaction resistance curves, which describe the relationship between the cyclic stress ratio (CSR) and the vibration number of failure (N_L). Different CSRs were applied to samples, resulting in different vibration numbers of failure; thus, liquefaction resistance curves are also called CSR–N_L curves. Before the test, the samples were divided into nine groups according to dry density and consolidation confining pressure. Each group contains seven or eight samples, and different cyclic loads (different CSRs) were applied to samples of the same group during the test. The failure criterion was liquefaction of the test sample, that is, the pore water pressure reached the confining pressure. In processing the test results, test samples with obvious deviations due to factors such as uneven sample preparation or insufficient saturation were discarded. Five valid test datasets were obtained under each confining pressure condition. Therefore, the CSR-N_L curves of each group of samples were fitted by 15 data points from three different consolidation confining pressures to ensure that the experimental results were representative.

In addition to the liquefaction resistance, the dynamic shear modulus G_d and damping ratio λ are two important parameters that describe the dynamic characteristics of the soil. They reflect changes in the stiffness and energy dissipation of the soil under a cyclic load. The values of G_d and λ can be calculated from the following equations:

$$G_d = \tau_d/\gamma_d \tag{4}$$

$$\lambda = A_{loop}/4\pi A_{\Delta} \tag{5}$$

where τ_d is the dynamic shear stress, γ_d is the dynamic shear strain, A_{loop} is the area of the enclosed hysteresis loop, and A_{Δ} is the area of the triangle under the line connecting the origin to the maximum amplitude point (Cao et al. 2020).

Unlike the liquefaction resistance test, the loading method to obtain G_d and λ is level-by-level loading, and the load in each level is cycled five times. To eliminate the effect of the dynamic pore pressure of the previous cycle load, the drain valve was quickly opened and closed once after each cycle load was completed, and then, the next cycle load was continued. Moreover, the initial dynamic shear modulus G_{d0} (also known as the maximum dynamic shear modulus G_{dmax}) generally refers to the dynamic shear modulus G_d when the shear strain reaches 0.001%. However, conventional dynamic triaxial instruments generally cannot collect such small strain

values owing to insufficient measurement accuracy. Geotechnical researchers and engineers have found alternative methods to determine the low-strain shear modulus. The maximum dynamic shear modulus G_{d0} can be calculated from the shear wave velocity (Hardin and Richart 1963). Based on this principle, the bending element method has become one of the methods commonly used in laboratories to determine G_{d0}, which was confirmed and applied in many engineering studies (Akin et al. 2011; Cao et al. 2019). G_d is calculated by the following equation:

$$G_{d0} = \rho V_s^2 \tag{6}$$

where ρ is the density of the sample and V_s is the shearing wave velocity.

In this experiment, G_{d0} was obtained using a bending element test module combined with a GDS Dynamic Triaxial Testing System.

Results and discussion

Compression behavior

The normal compression curves (e-p curves) of PG are depicted in Fig. 3. A large deformation appears in samples with all three dry densities. Moreover, after applying a pressure of 3200 kPa for 24 h, the deformation of the samples is still significant and tends to continue to increase, which indicates that PG has a significant creep characteristic. The vertical pressure in the consolidation test not only pushes the particles in the PG samples closer together but also deforms or even destroys the crystal structure of the PG. The destroyed PG crystal structure needs a longer time for rearrangement to reach stability again (Mi et al. 2015). According to the China national standard "Code for investigation of geotechnical engineering" (GB 50021-2001), Table 3 lists the reference value for classifying the compressibility and permeability of soil. The compressibility parameters of PG are shown in Table 4, and it can be confirmed that PG is moderately compressible.

Permeability behavior

The permeability coefficient (k) test results of PG with three dry densities are shown in Table 5. The permeability coefficient of PG decreases with increasing dry density, and according to the reference value for permeability classification shown in Table 3, the permeability gradually changes from moderate to weak. Thus, increasing the stacking density can effectively restrict the leachate from penetrating the substrate, reducing the environmental pollution from PG ponds.

Table 3 Reference values for classifying the compressibility and permeability of soil

Compressibility classification			Permeability classification	
Degree	Compression coefficient a_v (MPa^{-1})	Compression modulus E_s (MPa)	Degree	Permeability coefficient k (m/s)
High	> 0.5	< 4	Strong	10^{-4}–10^{-2}
Medium	0.1–0.5	4–20	Medium	10^{-6}–10^{-4}
Low	< 0.1	> 20	Weak	10^{-7}–10^{-6}
			Tiny	10^{-8}–10^{-7}

Triaxial shear properties

The triaxial shear test results, including the stress-strain curves, deformation modulus, peak stress, and shear strength parameters, are shown in Fig. 4.

Stress-strain curves

The stress-strain curves of the PG samples with the three investigated dry densities are depicted in Fig. 4a. The stress-strain relation can be divided into three deformation stages.

Stage 1: Initial deformation stage (linear strain hardening stage). This stage occurs at the initial deformation, and the sample strain is less than 1%. The stress-strain curve rises linearly, and the stress of the sample increases rapidly. When the samples have a higher dry density or confining pressure, the slope of the curve is steeper, and the duration of this stage is shorter. In this stage, the stress-strain curve of the PG exhibits a linear elastic relationship, which can be characterized by the deformation modulus of the samples.

Stage 2: Strain hardening stage (nonlinear strain hardening stage). The stress continues to increase with increasing strain. However, the slope of the curve gradually decreases as the strain increases, and the curve bends downward until it gradually approaches a horizontal line. The deformation modulus gradually decays to 0 when the peak stress is reached, which is similar to the previous stage. As the dry density and confining pressure of the samples increase, the duration of this stage is lengthened, implying that the samples may consume more energy to achieve the same deformation.

Stage 3: Destruction stage (zero-deformation modulus stage). In this stage of the stress-strain curve, the strain of the samples continues to increase but the stress remains unchanged, following the peak stress. That is, the deformation modulus remains almost zero.

Deformation modulus

The deformation modulus is defined as the ratio of a stress increment to the corresponding strain increment during a static triaxial test and is one of the important indexes for calculating the deformation of dam settlement. In this paper, the symbol E (MPa) refers to the deformation modulus corresponding to the initial deformation stage of a stress-strain curve.

The impact of confining pressure on the deformation modulus is depicted in Fig. 4b. It can be observed that the deformation modulus of PG is positively correlated with the dry density and confining pressure. Through a quantitative analysis of the effect of confining pressure, a notable result is that the value of the deformation modulus does not simply increase linearly. For test groups L1 and L2, the deformation modulus is linearly related to the confining pressure. These relationships can be described by the following two regression expressions:
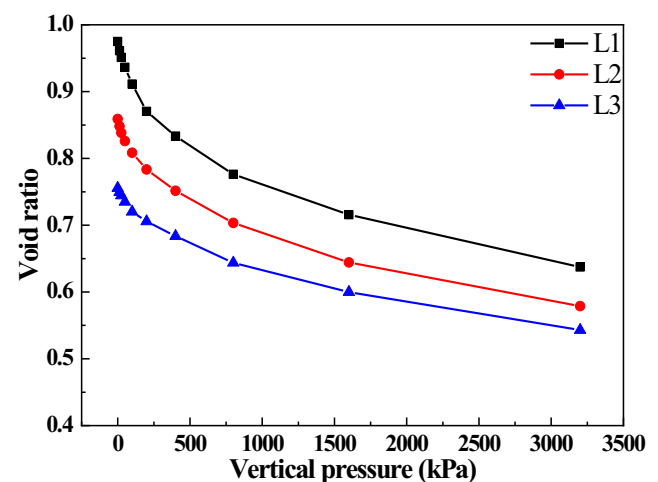
Table 4 Compressibility parameters of phosphogypsum

Test group	Compression coefficient a_v (MPa^{-1})	Compression modulus E_s (MPa)
L1	0.409	4.575
L2	0.251	7.107
L3	0.145	11.776

Fig. 3 Compression curves of phosphogypsum

Table 5 Permeability coefficients of phosphogypsum

Test group	Maximum value (m/s)	Minimum value (m/s)	Average value (m/s)
L1	5.08×10^{-5}	1.25×10^{-5}	2.97×10^{-5}
L2	6.01×10^{-6}	4.27×10^{-6}	5.03×10^{-6}
L3	9.26×10^{-7}	6.20×10^{-7}	8.22×10^{-7}

$$E_{L1} = 15.77 + 0.16\sigma_3 \tag{7}$$

with a goodness of fit $R^2 = 0.9871$. In Eqs. (7) to (10), E is the deformation modulus (MPa) and σ_3 is the confining pressure (kPa).

$$E_{L2} = 10.17 + 0.27\sigma_3 \tag{8}$$

with a goodness of fit $R^2 = 0.9996$.

However, in group L3, the logarithmic relationship has a higher correlation coefficient than the linear relationship. The curve fitting obtained the following expressions.

For the linear fitting,

$$E_{L3} = 62.59 + 0.16\sigma_3 \tag{9}$$

with a goodness of fit $R^2 = 0.8744$

For the logarithmic fitting,

$$E_{L3} = 59.42\ln(\sigma_3) - 224.55 \tag{10}$$

with a goodness of fit $R^2 = 0.9556$

Equations (7) to (10) show that within the range of experimental conditions, as the dry density increases, the relationship between the deformation modulus and confining pressure gradually changes from a linear relationship to a logarithmic relationship. The reason for this property of PG is that the greater the dry density of the sample is, the stronger the connection between the PG particles, which will cause the consolidation of the confining pressure to have less of an effect on the sample.
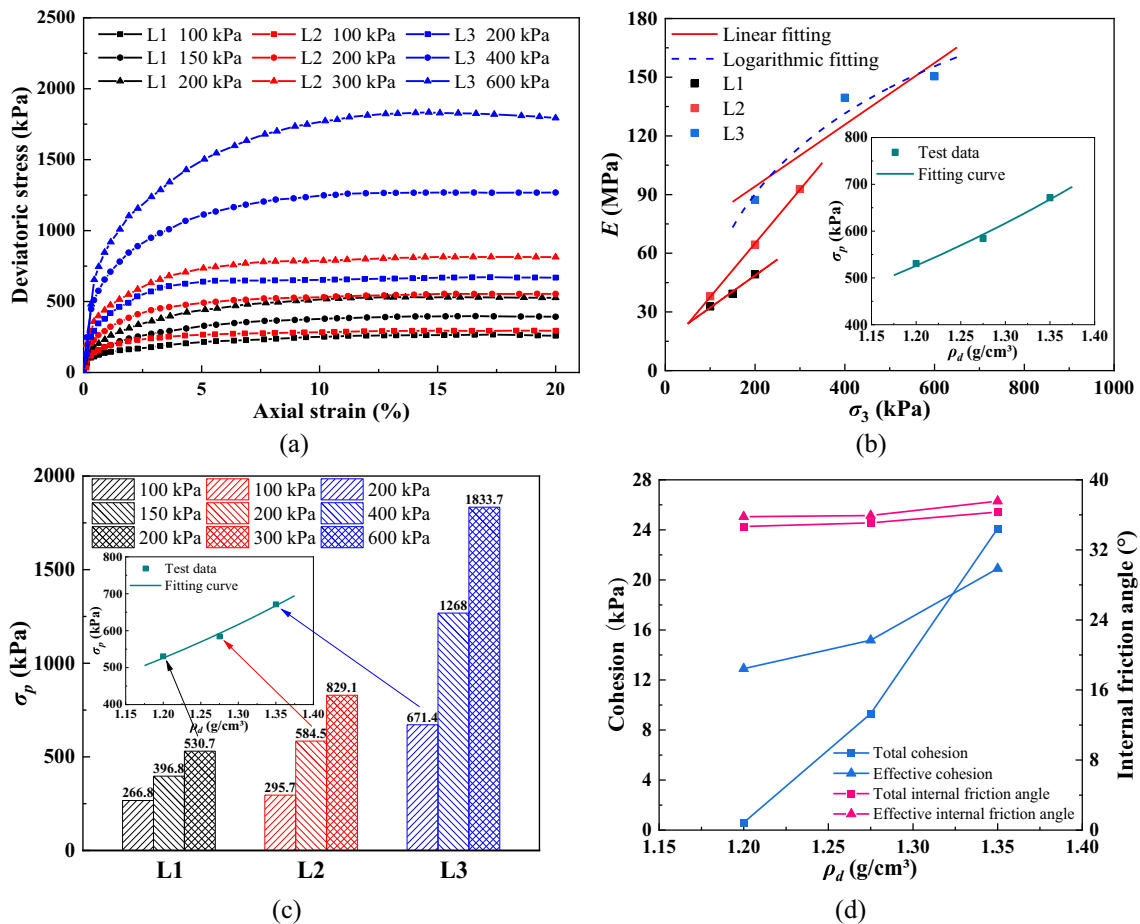

Fig. 4 Triaxial shear test results of phosphogypsum. **a** Stress-strain curves. **b** Deformation modulus. **c** Peak stress. **d** Shear strength parameters

The effect of dry density on deformation modulus was investigated under the same confining pressure of 200 kPa, as presented in Fig. 4b. This figure indicates that the deformation modulus of PG is exponentially related to its dry density. This relationship can be described by the following regression expression:

$$E = 0.47e^{3.86\rho_d} \tag{11}$$

with a goodness of fit $R^2 = 0.9990$, where E is the deformation modulus (MPa) and ρ_d is the dry density (g/cm^3).

Shear strength

Shear strength is usually described by the peak stress (σ_p) and shear strength parameters. Figure 4 c depicts the change in peak stress with changing dry density. Clearly, with increasing dry density and consolidation confining pressure, the peak stress of the samples increased from 266.8 to 1833.7 kPa. To study the effect of the dry density of PG on the peak stress, the results of each group of samples under 200 kPa of confining pressure were normalized; this change was fitted by the following expression:

$$\sigma_p = 78.0731e^{1.5898\rho_d} \tag{12}$$

with a goodness of fit, $R^2 = 0.9899$, where σ_p is the peak stress (kPa) and ρ_d is the dry density (g/cm^3).

Equation (12) shows that peak stress is exponentially related to dry density. This is because the void ratio of a test sample with a higher dry density is correspondingly lower. Additionally, the effective contact area between particles increases with increasing dry density, thereby increasing the strength of the test sample (Zheng et al. 2019).

According to the Mohr-Coulomb criterion, the shear strength parameters of PG can be calculated by fitting the peak stresses of each group of samples under the three tested confining pressures to the strength envelope, and the results are shown in Fig. 4d. The shear strength parameters—either the total shear strength parameters (c and φ) or the effective shear strength parameters (c' and φ')—also increase with increasing dry density. The increase in cohesion (c and c') is more significant than that of the internal friction angle. This is because the cohesion of the soil depends on various physical and chemical forces between the soil particles. As the density of the samples increases, the distance between the PG particles decreases, resulting in more contact points for particles per unit area; therefore, the cohesion increases. However, the change in the internal friction angle (φ and φ') with density is relatively small. It is well known that the internal friction angle of soil reflects the friction characteristics of the soil and is generally considered to include two parts: the surface

friction of soil particles and the interparticle bite force. The SEM results show that the PG particles are rhombic and prismatic and are more regular and smoother than the irregular shapes of particles of soil and conventional tailings (Tayibi et al. 2009). This obfuscates the friction effect on the surface of the particles and the interaction between the particles. Therefore, even if the physical states of the samples are different, the internal friction angle of PG does not change significantly.

Dynamic properties

The liquefaction resistance, dynamic shear modulus, and damping ratio of PG with different dry densities or confining pressures are shown in Fig. 5.

Liquefaction resistance

The liquefaction resistance curves (CSR-N_L curves) of the PG samples with the three investigated dry densities are depicted in Fig. 5a. Clearly, the trends of the CSR-N_L curves of PG with different dry densities are consistent. For the same group of samples, with increasing CSR, the number of vibrations required for the samples to fail gradually decreases, and their relationship could be fitted using the following power function:

$$CSR = aN_L{}^b \tag{13}$$

where coefficient a is equivalent to the CSR that produces liquefaction in one loading cycle (that is, the CSR when $N_L = 1$) and exponent b reflects the relationship between the soil characteristics and CSR (Riveros and Sadrekarimi 2020). The fitting parameters and goodness of fit of the PG samples with different dry densities are summarized in Fig. 5a. The goodness of fit of the power functions are all greater than 0.95, indicating a high degree of fit. The CSRs under different confining pressures can be well normalized, indicating that it is appropriate to reflect the anti-liquefaction performance of PG with CSR, and the result is not affected by confining pressure conditions. In addition, among the samples with the different dry densities, a sample with a higher dry density requires more vibrations to fail. The samples that exhibit higher a coefficients have CSR-N_L curves that are shifted to higher positions. They also exhibit relatively larger b exponents, which implies that the CSR-N_L curves of the samples with higher dry density are steeper. Regardless of the distribution of the curves or the fitting parameters, the samples with higher dry density demonstrate better liquefaction resistance.

Dynamic shear modulus

The dynamic shear modulus G_d reflects the ability of soil to resist shear strain under cyclic loading and the dynamic shear stress–shear strain relationship during the elastic deformation
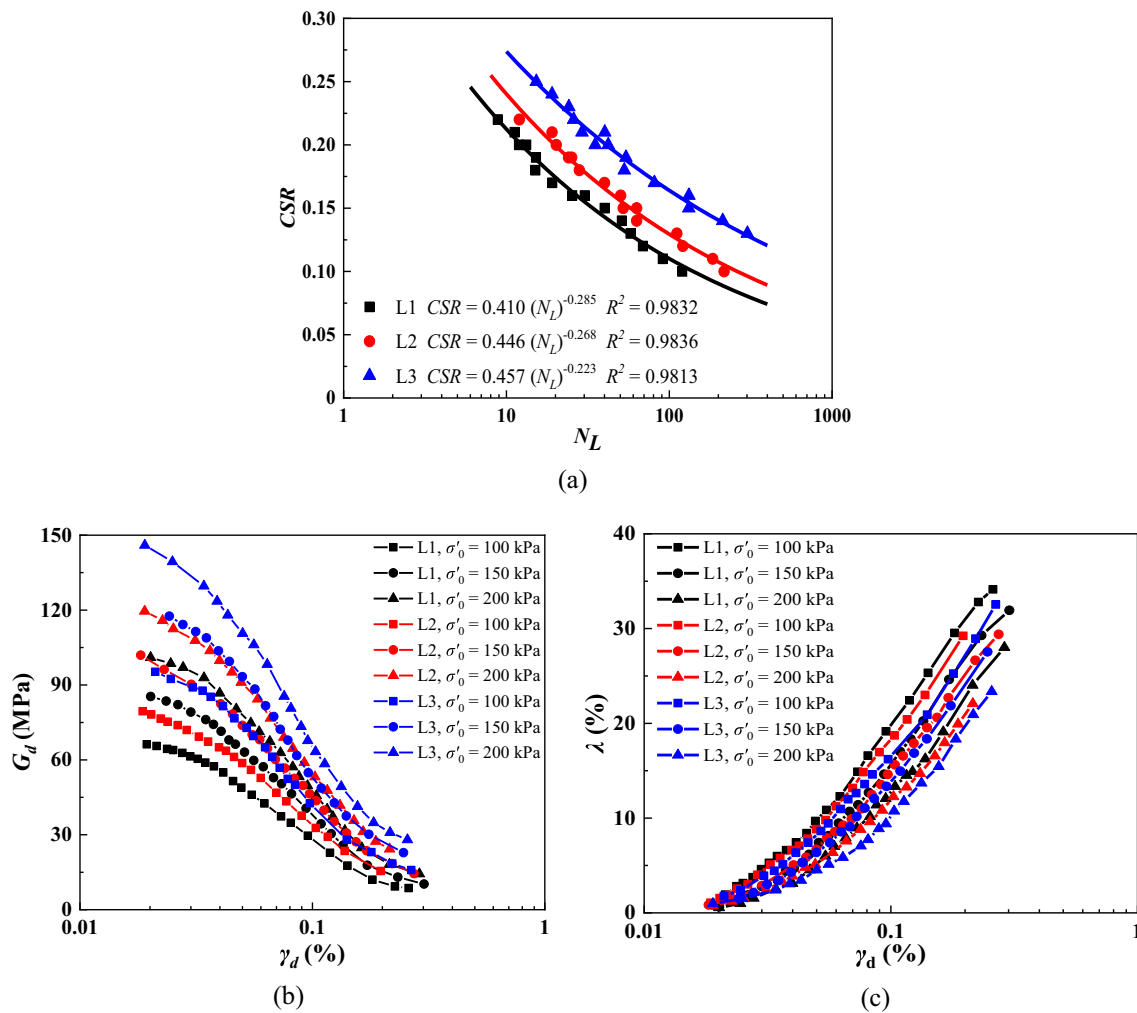
(a)

(b)

(c)

Fig. 5 Dynamic triaxial test results of phosphogypsum. **a** Liquefaction resistance curves. **b** Dynamic shear modulus. **c** Damping ratio

stage. The results of the bending element tests, including the sample saturation density and shear wave velocity, of the samples with three different dry densities under different
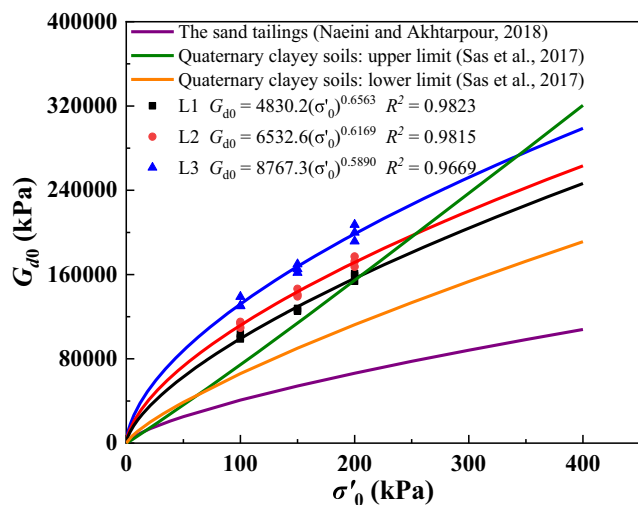

Fig. 6 Initial dynamic shear modulus of PG and other materials

stress states are substituted into Eq. (6) according to the elastic wave theory. The initial dynamic shear modulus G_{d0} of PG is depicted in Fig. 6. Clearly, the values of G_{d0} increase with increasing dry density and effective consolidation confining pressure. This is because a sample with a higher dry density or confining pressure has a smaller void ratio. The void ratio significantly influences the shear wave velocity V_s, which can be expressed as a power function relationship (Cao et al. 2019). The test results for each density were fitted, and the relationship between the stress state and initial dynamic shear modulus G_{d0} was analyzed. The fitting equations for the initial dynamic shear modulus G_{d0} of PG with different dry densities are shown in Fig. 6. The results demonstrate that the mean effective stress σ_0' and initial dynamic shear modulus G_{d0} exhibit a power relationship, which can be expressed by Eq. (14).

$$G_{d0} = \alpha \left(\sigma_0' \right)^\beta \tag{14}$$

where α and β are two parameters that reflect the

characteristics of the soil and σ_0' is the mean effective confining pressure.

Similar conclusions were obtained by Naeini and Akhtarpour (2018) and Sas et al. (2017) who carried out research on sand tailings and Quaternary clayey soils, respectively. According to Pineda et al. (2014), these equations could be used for determining G_{d0} at different stress states. It can also be seen in Fig. 6 that the initial dynamic shear modulus of PG is higher than those of sand tailings and Quaternary clay under most conditions and is lower than the upper limit of Quaternary clay only when the effective confining pressure is greater than 350 kPa.

Based on the dynamic triaxial test results, the dynamic shear moduli of the PG samples with different dry densities are depicted in Fig. 5b for different confining pressures. The change rules of the dynamic shear modulus G_d of different groups of samples are basically the same: G_d decreases with increasing shear strain and increases with increasing dry density and consolidation confining pressure.

To conveniently describe the change law of the dynamic shear modulus under different confining pressures, Hardin and Drnevich (1972) proposed the concept of the dynamic shear modulus ratio, which is the ratio of the dynamic shear modulus to the initial dynamic shear modulus. This process is equivalent to normalizing the test data under different confining pressures. In this study, the Hardin–Drnevich model (Eq. (15)) and the Davidenkov model (Eq. (16)) were used to fit the test results of PG samples with different dry density.

$$\frac{G_d}{G_{d0}} = \frac{m}{1 + (\gamma_d/\gamma_{c1})} \tag{15}$$

$$\frac{G_d}{G_{d0}} = 1 - \left[\frac{(\gamma_d/\gamma_{c2})^{2B}}{1 + (\gamma_d/\gamma_{c2})^{2B}}\right]^A \tag{16}$$

where γ_d is the dynamic shear strain and m, A, B, γ_{c1}, and γ_{c2} are the fitting parameters related to the soil properties. Among them, m, A, and B are dimensionless, and γ_{c1} and γ_{c2} are the corresponding strains in the same unit as γ_d.

The fitting results are shown in Table 6. The correlation coefficients of the two models for each group of samples are greater than 0.95, indicating that both models are suitable for PG.

The relationship between the dynamic shear modulus ratio G_d/G_{d0} and the dynamic shear strain γ_d of PG is depicted in
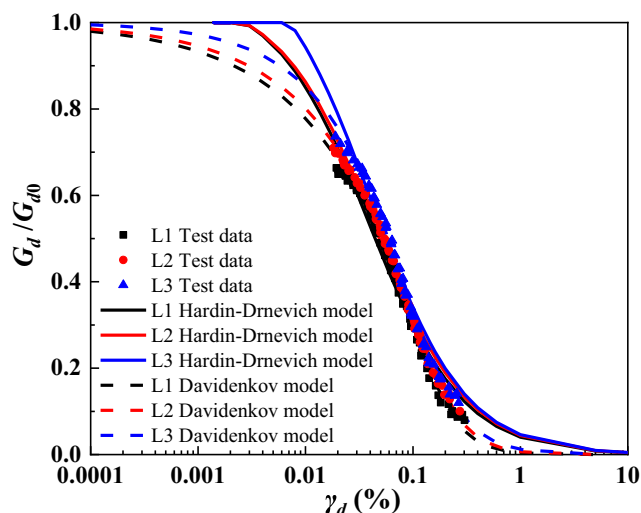

Fig. 7 Curves of the dynamic shear modulus ratio vs dynamic shear strain

Fig. 7. When the dynamic shear modulus ratio corresponding to a certain strain is equal to 1, the dynamic shear modulus corresponding to this strain is equal to the initial dynamic shear modulus. The soil is in the stage of elastic deformation at this time, and the corresponding dynamic shear strain is often less than 0.001% (Seed et al. 1986). Using the Hardin–Drnevich model, the strain is only 0.01% when the dynamic shear modulus ratio reaches 1. However, for the Davidenkov model, the strain must be less than 0.001%, or even less than 0.0001%. The results of both models demonstrate that when the modulus ratio decreases to approximately 0.3, the modulus ratio curve begins to decrease rapidly. The difference is that the decline rate of the curve of the Hardin–Drnevich model is slower than that of the Davidenkov model. This leads to shear strains of 1% for the Davidenkov model and 10% for the Hardin–Drnevich model when the modulus ratio is reduced to zero. The modulus is an index used to describe the degree of difficulty of deformation of the material. A modulus ratio of zero means that the sample has no resistance to deformation. Once subjected to external force, the sample is easily damaged. In this study, the failure form of the sample is liquefaction. The PG sample results in the liquefaction resistance test suggest that the shear strain at sample failure is not more than 1%. At this time, the PG specimen completely loses its resistance to deformation; that is, when the dynamic shear strain is approximately 1%, the corresponding dynamic shear modulus is 0, which is closer to the

Table 6 Fitting parameters of the dynamic shear modulus ratios for phosphogypsum

Test group	Hardin–Drnevich model			Davidenkov model			
	m	γ_{c1}	R^2	A	B	γ_{c2}	R^2
L1	1.0689	3.91×10^{-4}	0.9711	0.2209	1.1813	1.79×10^{-3}	0.9956
L2	1.0620	4.33×10^{-4}	0.9776	0.2639	1.0714	1.74×10^{-3}	0.9974
L3	1.1741	4.08×10^{-4}	0.9753	0.4090	0.8920	1.36×10^{-3}	0.9942

Fig. 8 Comparison of modulus ratio ranges between PG and other geotechnical materials
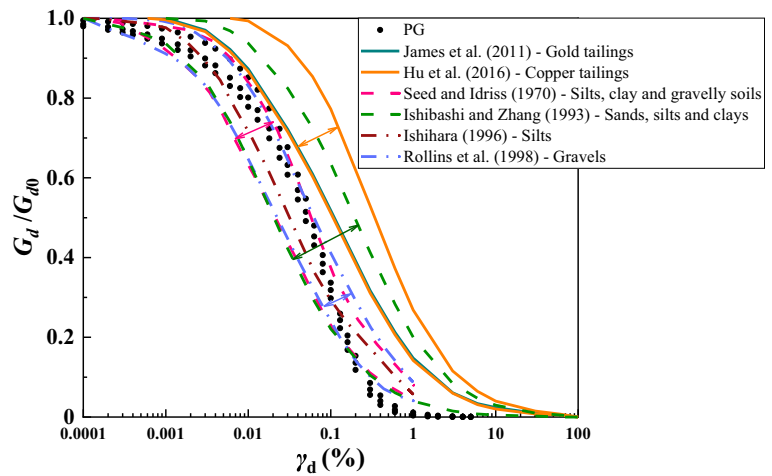
prediction result of the Davidenkov model. Therefore, we believe that the Davidenkov model is more reasonable than the Hardin–Drnevich model for PG analysis.

As shown in Fig. 8, to compare the differences and similarities between PG and other geotechnical materials, the relationship between the dynamic shear modulus ratios and shear strain in this study is compared with the results presented in some classic studies. Compared with the test results of James et al. (2011) and Hu et al. (2017), our test results of PG plot lower than those of gold tailings and copper tailings, which also means that the PG is less resistant to deformation. Compared with conventional soil, in which the shear strain is less than 0.3%, the modulus ratio curve of PG is within the ranges presented by Seed and Idriss (1970), Ishibashi and Zhang (1993), Ishihara (1996), and Rollins et al. (1998), but when the shear strain is greater than 0.3%, the dynamic shear modulus is greatly reduced and lower than these test ranges, reflecting the characteristic that PG is more easily deformed after responding to a high shear strain.

Damping ratio

The damping ratio (λ) of soil is an important indicator of the energy consumption of the soil under cyclic dynamic loads, which reflects the nature of energy loss due to the internal resistance of the soil under dynamic loading. The damping ratio is also an important manifestation of the hysteresis of the

dynamic stress-strain relationship of soil under dynamic loading. According to the definition of the damping ratio (λ), the damping ratio is calculated from the area of the hysteresis loop. The damping ratio (λ) results of PG are depicted in Fig. 5c, which shows that the damping ratios obtained in each group of tests are similar. As the shear strain increases, the damping ratio first increases gradually and then increases extremely rapidly. At the same dry density, the damping ratio decreases with increasing confining pressure. Under the same consolidation confining pressure, the higher the dry density is, the smaller the damping ratio. The influence of confining pressure and dry density on the damping ratio of PG is observed to be significant.

In view of the accuracy limitations of the test equipment, the damping ratio obtained in the tests corresponds only to the shear strain range of 0.01 to 1%, which cannot fully reflect the damping ratio characteristics of PG. In previous studies, a formula based on dynamic shear modulus ratio test results was commonly used to calculate the damping ratio. Table 7 presents the commonly used formulas for calculating the damping ratio.

The four formulas in Table 7 can be unified into the following formula:

$$\lambda = k_1 (G_d/G_{d0})^2 + k_2 (G_d/G_{d0}) + k_3 \quad (17)$$

where k_1, k_2, and k_3 are the model parameters, and G_d/G_{d0} can be determined with dynamic shear modulus test results.

In this study, Eq. (17) is used to fit the change in the PG damping ratio. Considering that the confining pressure has a

Table 7 Empirical formulas of damping ratios

Serial number	Calculation formula	Test material	Scholars and reports
1	$\lambda = 0.333[0.586(G_d/G_{d0})^2 - 1.547(G_d/G_{d0}) + 1]$	Sands	Ishibashi and Zhang (1993)
2	$\lambda = a[b(G_d/G_{d0})^2 - c(G_d/G_{d0}) + 1]$	Plastic and non-plastic soils	Park (1998)
3	$\lambda - \lambda_{min} = 10.6(G_d/G_{d0})^2 - 31.6(G_d/G_{d0}) + 21.0$	Residual and saprolite soils	Zhang et al. (2005)
4	$\lambda = 20.4(G_d/G_{d0} - 1)^2 + 3.1$	Piedmont residual soils	Borden et al. (1996)

Table 8 Fitting parameters of the phosphogypsum damping ratio

Test group	Mean effective confining pressure (kPa)	Fitting result			
		k_1	k_2	k_3	R^2
L1	100	0.2556	− 0.7272	0.3922	0.9996
	150	0.4007	− 0.7868	0.3573	0.9988
	200	0.4552	− 0.7583	0.3123	0.9946
L2	100	0.2622	− 0.6971	0.3683	0.9989
	150	0.3859	− 0.7335	0.3331	0.9980
	200	0.3522	− 0.6258	0.2737	0.9975
L3	100	0.3450	− 0.7387	0.3600	0.9949
	150	0.4015	− 0.7292	0.3221	0.9970
	200	0.4437	− 0.6969	0.2882	0.9953

significant effect on the damping ratio of soil, to make the fitting result better reflect the changing trend of the PG damping ratio, the influence of the consolidation confining pressure is considered in addition to the density. The fitting process analyzes the samples with different confining pressures in each group of tests. The results are presented in Table 8. The goodness of fit results are greater than 0.95, indicating that the applicability of the model is good.

Figure 9 depicts a comparison of the test results of the PG damping ratio with the test ranges presented in some classic literature (Seed and Idriss 1970; Ishihara 1996; Rollins et al. 1998). By comparison, it is found that when the shear strain is greater than 0.1%, many test points of the PG damping ratio determined in this work are higher than the results of other studies. This shows that PG has a high energy dissipation characteristic under the condition of a high shear strain; thus, PG is easily liquified because the pore water pressure potential energy rises quickly.
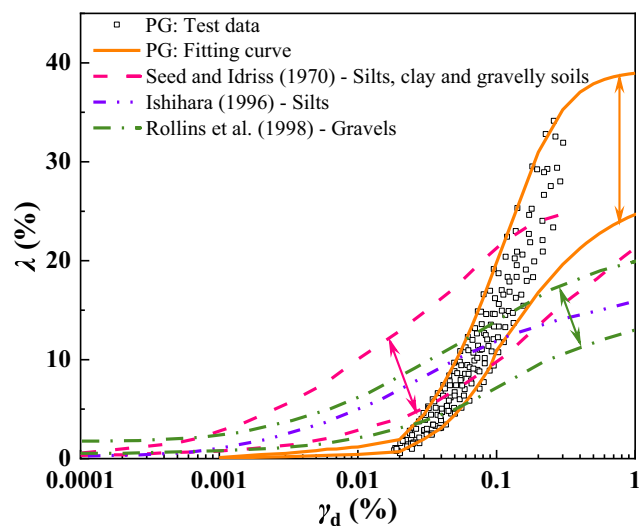

Fig. 9 Comparison of damping ratio ranges between PG and other geotechnical materials

Conclusion

This study is a systematic assessment of the static and dynamic mechanical properties of PG. The results show that the phosphogypsum had medium compressibility and medium to weak permeability (with increasing dry density). The stress-strain curve of PG under triaxial shear was divided into three typical stages. With increasing dry density and consolidation confining pressure, the peak stress, shear strength parameters (cohesion and internal friction angle), and deformation modulus of PG all increased. The peak stress and deformation modulus of PG were exponentially related to the dry density. As the dry density increased, the relationship between the deformation modulus and confining pressure gradually changed from linear to logarithmic. The liquefaction resistance curves (CSR-N_L curves) of PG were expressed by power functions. The CSR–N_L curves under different confining pressures were well normalized. With increasing dry density, the curve shifted higher and became steeper. Compared with the Hardin–Drnevich model, the Davidenkov model was more suitable for describing the relationship between the dynamic shear modulus ratio and damping ratio of PG and the dynamic shear strain. Compared with the properties of tailings and natural soils, the initial dynamic shear modulus of PG was higher, and the dynamic shear stress of PG had a more significant effect on its dynamic shear modulus ratio and damping ratio. In summary, compared with soils, PG has relatively poor engineering mechanical properties, which may be related to its uniform particle distribution and neat particle stacking structure. Increasing the density of PG can improve its static and dynamic mechanical properties, which is meaningful for improving the stability and safety management of PG ponds.

ZW gives input for the structure of the manuscript as well as scientific advice and provided the funding support. YY interpreted the test data and proof-read the manuscript. GC helped to operate experimental equipment and demonstrated the feasibility of the scheme. All authors read and approved the final manuscript.

Data availability The datasets used and analyzed during the current study are available from the corresponding author on reasonable request.

Compliance with ethical standards

Ethics approval and consent to participate   Not applicable.

Consent for publication   Not applicable.

Competing interest   The authors declare that they have no competing interest.

Abbreviations   CU, triaxial consolidated-undrained test; CSR, cyclic stress ratio; N_L, vibration number of failures; ρ_d, dry density; ρ, wet density; D_{50}, average particle size; C_u, non-uniform coefficient; C_c, curvature coefficient; e, void ratio; p, vertical pressure; ε, axial strain; k, permeability coefficient; a_v, compression coefficient; E_s, compression modulus; E, deformation modulus; σ_p, peak stress; c (c'), total cohesion (effective cohesion); φ (φ'), total internal friction angle (effective internal friction angle); σ'_0, mean effective confining pressure; σ_1, σ_3, axial and radial consolidation pressure; σ_d, dynamic stress; μ_0, initial pore water pressure; τ_d, dynamic shear stress; γ_d, dynamic shear strain; A_{loop}, area of the enclosed hysteresis loop; $A_{\triangle}$, area of the triangle under the line connecting the origin to the maximum amplitude point; G_d, dynamic shear modulus; Λ, damping ratio; G_{d0} (G_{dmax}), initial dynamic shear modulus (maximum dynamic shear modulus); V_s, shearing wave velocity

References

Akin MK, Kramer SL, Topal T (2011) Empirical correlations of shear wave velocity (V_s) and penetration resistance (SPT-N) for different soils in an earthquake-prone area (Erbaa-Turkey). Eng Geol 119:1–17. https://doi.org/10.1016/j.enggeo.2011.01.007

ASTM international (2011a) Standard Test Method for Consolidated Undrained Triaxial Compression Test for Cohesive Soils (ASTM D4767-11).

ASTM international (2011b) Standard Test Method for One-Dimensional Consolidation Properties of Soils Using Incremental Loading (ASTM D2435/D2435M-11).

Borden RH, Shao L, Gupta A (1996) Dynamic properties of piedmont residual soils. J Geotech Eng 122:813–821. https://doi.org/10.1061/(asce)0733-9410(1996)122:10(813)

Bumanis G, Zorica J, Bajare D, Korjakins A (2018) Technological properties of phosphogypsum binder obtained from fertilizer production waste. Energy Procedia 174:301–308. https://doi.org/10.1016/j.egypro.2018.07.096

Canut MMC, Jacomino VMF, Bratveit K, Gomes AM, Yoshida MI (2008) Microstructural analyses of phosphogypsum generated by Brazilian fertilizer industries. Mater Charact 59:365–373. https://doi.org/10.1016/j.matchar.2007.02.001

Cao GS, Wang WS, Yin GZ, Wei ZA (2019) Experimental study of shear wave velocity in unsaturated tailings soil with variant grain size distribution. Constr Build Mater 228:116744. https://doi.org/10.1016/j.conbuildmat.2019.116744

Cao GS, Wei ZA, Wang WS, Zheng BB (2020) Shearing resistance of tailing sand waste pollutants mixed with different contents of fly ash. Environ Sci Pollut Res 27:8046–8057. https://doi.org/10.1007/s11356-019-07419-6

Chen QS, Zhang QL, Fourie A, Xin C (2017) Utilization of phosphogypsum and phosphate tailings for cemented paste backfill. J Environ Manage 201:19–27. https://doi.org/10.1016/j.jenvman.2017.06.027

Chen XM, Gao JM, Zhao YS (2019) Investigation on the hydration of hemihydrate phosphogypsum after post treatment. Constr Build Mater 229:116864. https://doi.org/10.1016/j.conbuildmat.2019.116864

Cuadri AA, Navarro FJ, Garcia-Morales M, Bolivar JP (2014) Valorization of phosphogypsum waste as asphaltic bitumen modifier. J Hazard Mater 279:11–16. https://doi.org/10.1016/j.jhazmat.2014.06.058

Escobar H (2015) Mud tsunami wreaks ecological havoc in Brazil: researchers analyze sludge for heavy metals and assess potential for recovery. Science 350:1138–1139. https://doi.org/10.1126/science.350.6265.1138

Geraldo RH, Costa ARD, Kanai J, Silva JS, Souza JD, Andrade HMC, Gonçalves JP, Fontanini PSP, Camarini G (2020) Calcination parameters on phosphogypsum waste recycling. Constr Build Mater 256:119406. https://doi.org/10.1016/j.conbuildmat.2020.119406

Gorbovskiy KG, Ryashko AI, Kazakov AI, Norov AM, Mikhaylichenko AI (2018) The influence of water-soluble impurities on thermal dehydration kinetics of phosphogypsum in self-generated atmosphere. J Therm Anal Calorim 133:1549–1562. https://doi.org/10.1007/s10973-018-7272-1

Hammas-Nasri I, Horchani-Naifer K, Férid M, Barca D (2019) Production of a rare earths concentrate after phosphogypsum treatment with dietary NaCl and Na_2CO_3 solutions. Miner Eng 132:169–174. https://doi.org/10.1016/j.mineng.2018.12.013

Hardin BO, Richart FE (1963) Elastic wave velocities in granular soils. J Soil Mech Found Div 89:33–65

Hardin BO, Drnevich VP (1972) Shear modulus and damping in soils: design equations and curves. J Soil Mech Found Div 98:667–692

Hu LM, Wu H, Zhang L, Zhang PW, Wen QB (2017) Geotechnical properties of mine tailings. J Mater Civ Eng 29:04016220. https://doi.org/10.1061/(ASCE)MT.1943-5533.0001736

Hudson-Edwards K (2016) Tackling mine wastes: global collaboration is needed to mitigate the environmental impacts of mine wastes. Science 352:288–290. https://doi.org/10.1126/science.aaf3354

Ishibashi I, Zhang XJ (1993) Unified dynamic shear moduli and damping ratios of sand and clay. Soils Found 33:182–191. https://doi.org/10.3208/sandf1972.33.182

Ishihara K (1996) Soil behavior in earthquake geotechnics. Oxford University Press, Great Britain

Ishihara K, Ueno K, Yamada S, Yasuda S, Yoneoka T (2015) Breach of a tailings dam in the 2011 earthquake in Japan. Soil Dyn Earthq Eng 68:3–22. https://doi.org/10.1016/j.soildyn.2014.10.010

Jalali J, Gaudin P, Capiaux H, Ammar E, Lebeau T (2019) Fate and transport of metal trace elements from phosphogypsum piles in Tunisia and their impact on soil bacteria and wild plants. Ecotox Environ Safe 174:12–25. https://doi.org/10.1016/j.ecoenv.2019.02.051

James M, Aubertin M, Wijewickreme D, Wilson GW (2011) A laboratory investigation of the dynamic properties of tailings. Can Geotech J 48:1587–1600. https://doi.org/10.1139/T11-060

Kammoun M, Ghorbel I, Charfeddine S, Kamoun L, Gargouri-Bouzid R, Nouri-Ellouz O (2017) The positive effect of phosphogypsum-

supplemented composts on potato plant growth in the field and tuber yield. J Environ Manage 200:475–483. https://doi.org/10.1016/j.jenvman.2017.06.016

Li B, Wei S, Zhen YW (2020) An effective recycling direction of water-based drilling cuttings and phosphogypsum co-processing in road cushion layer. Environ Sci Pollut Res 27:17420–17424. https://doi.org/10.1007/s11356-020-08406-y

Ma BG, Lu WD, Su Y, Li YB, Gao C, He XY (2018) Synthesis of α-hemihydrate gypsum from cleaner phosphogypsum. J Clean Prod 195:396–405. https://doi.org/10.1016/j.jclepro.2018.05.228

Mi ZK, Rao XS, Chu XQ, Cao P (2015) Physico-mechanical properties of deposition phosphogypsum. Chin J Geotech Eng 37:470–478 (in Chinese). https://doi.org/10.11779/CJGE201503010

Min CD, Li XB, He SY, Zhou ST, Zhou YA, Yang S, Shi Y (2019) Effect of mixing time on the properties of phosphogypsum-based cemented backfill. Constr Build Mater 210:564–573. https://doi.org/10.1016/j.conbuildmat.2019.03.187

Ministry of Construction of the People's Republic of China (2001) Code for investigation of geotechnical engineering (GB 50021-2001) (in Chinese).

Ministry of Emergency Management of the People's Republic of China (2017) Notice of the state administration of safety supervision on strengthening the safety production of phosphogypsum storage. https://www.mem.gov.cn/gk/gwgg/gfxwj/2017/201701/t20170123_242771.shtml

Ministry of Housing and Urban-Rural Development of the People's Republic of China, State Administration for Market Regulation (2019) Standard for geotechnical test method (GB/T 50123-2019) (in Chinese).

Naeini M, Akhtarpour A (2018) Numerical analysis of seismic stability of a high centerline tailings dam. Soil Dyn Earthq Eng 107:179–194. https://doi.org/10.1016/j.soildyn.2018.01.019

Papanicolaou F, Antoniou S, Pashalidis I (2009) Experimental and theoretical studies on physico-chemical parameters affecting the solubility of phosphogypsum. J Environ Radioact 100:854–857. https://doi.org/10.1016/j.jenvrad.2009.06.012

Park D (1998) Evaluation of dynamic soil properties: strain amplitude effects on shear modulus and damping ratio. Cornell University

Pineda JA, Colmenares JE, Hoyos LR (2014) Effect of fabric and weathering intensity on dynamic properties of residual and saprolitic soils via resonant column testing. Geotech Test J 37:20120132. https://doi.org/10.1520/GTJ20120132

People's government of Guizhou province. (2016) Notification about the "8·11" accident of Longjingwan phosphogypsum pond of Guizhou Kailing Group Mineral Fertilizer Co., Ltd. http://www.guizhou.gov.cn/zwgk/zdlygk/aqsc/cljcyjz/201709/t20170925_828673.html

Rashad AM (2017) Phosphogypsum as a construction material. J Clean Prod 166:732–743. https://doi.org/10.1016/j.jclepro.2017.08.049

Riveros GA, Sadrekarimi A (2020) Liquefaction resistance of Fraser River sand improved by a microbially-induced cementation. Soil Dyn Earthq Eng 131:106034. https://doi.org/10.1016/j.soildyn.2020.106034

Rollins KM, Evans MD, Diehl NB, Daily WD III (1998) Shear modulus and damping relationships for gravels. J Geotech Geoenviron Eng 5:396–405. https://doi.org/10.1061/(ASCE)1090-0241(1998)124:5(396)

Rychkov VN, Kirillov EV, Kirillov SV, Semenishchev VS, Bunkov GM, Botalov MS, Smyshlyaev DV, Malyshev AS (2018) Recovery of rare earth elements from phosphogypsum. J Clean Prod 196:674–681. https://doi.org/10.1016/j.jclepro.2018.06.114

Sas W, Gabryś K, Szymański A (2017) Experimental studies of dynamic properties of Quaternary clayey soils. Soil Dyn Earthq Eng 95:29–39. https://doi.org/10.1016/j.soildyn.2017.01.031

Seed HB, Idriss IM (1970) Soil module and damping factors for dynamic response analysis. EERC, Report No.70-10. University of California, Berkeley.

Seed HB, Wong RT, Idriss IM, Tokimatsu K (1986) Moduli and damping factors for dynamic analyses of cohesionless soils. J Geotech Eng 112:1016–1032. https://doi.org/10.1061/(ASCE)0733-9410(1986)112:11(1016)

Shen W, Gan G, Dong R, Chen H, Tan Y, Zhou M (2012) Utilization of solidified phosphogypsum as Portland cement retarder. J Mater Cycles Waste Manag 14:228–233. https://doi.org/10.1007/s11356-020-08406-y

State Administration for Market Regulation of the People's Republic of China (2018) Phosphogypsum (GB/T 23456-2018) (in Chinese).

State Administration of Work Safety of the People's Republic of China (2016) Safety technical regulation on phosphogypsum stack (AQ 2059-2016) (in Chinese).

Tayibi H, Choura M, Lopez FA, Alguacil FJ, Lopez-Delgado A (2009) Environmental impact and management of phosphogypsum. J Environ Manage 90:2377–2386. https://doi.org/10.1016/j.jenvman.2009.03.007

Tian T, Yan Y, Hu ZH, Xu YY, Chen YP, Shi J (2016) Utilization of original phosphogypsum for the preparation of foam concrete. Constr Build Mater 115:143–152. https://doi.org/10.1016/j.conbuildmat.2016.04.028

Wang T, Zhou Y, Lv Q, Zhu Y, Jiang C (2011) A safety assessment of the new Xiangyun phosphogypsum tailings pond. Miner Eng 24:1084–1090. https://doi.org/10.1016/j.mineng.2011.05.013

Wei Z, Yin G, Wang JG, Wan L, Li G (2013) Design, construction and management of tailings storage facilities for surface disposal in China: case studies of failures. Waste Manage Res 31:106–112. https://doi.org/10.1177/0734242X12462281

Wu S, Yao X, Ren C, Yao Y, Wang W (2020) Recycling phosphogypsum as a sole calcium oxide source in calcium sulfoaluminate cement and its environmental effects. J Environ Manage 271:110986. https://doi.org/10.1016/j.jenvman.2020.110986

Yang YH, Wei ZA, Fourie A, Chen YL, Zheng BB, Wang WS, Zhuang SN (2019) Particle shape analysis of tailings using digital image processing. Environ Sci Pollut Res 26:26397–26403. https://doi.org/10.1007/s11356-019-05974-6

Zeng LL, Bian X, Zhao L, Wang YJ, Hong ZS (2020) Effect of phosphogypsum on physiochemical and mechanical behaviour of cement stabilized dredged soil from Fuzhou, China. Geomech Energy Envir 100195. https://doi.org/10.1016/j.gete.2020.100195

Zhang C, Yang CH, Yu KJ, Fu SW, Chen F (2007) Study on physico-mechanical characteristics of phosphogypsum. Rock Soil Mech 28:461–466 (in Chinese). https://doi.org/10.16285/j.rsm.2007.03.006

Zhang JF, Andrus RD, Juang CH (2005) Normalized shear modulus and material damping ratio relationships. J Geotech Geoenviron Eng 131:453–464. https://doi.org/10.1061/(asce)1090-0241(2005)131:4(453)

Zheng BB, Zhang DM, Liu WS, Yang YH, Yang H (2019) Use of basalt fiber-reinforced tailings for improving the stability of tailings dam. Materials 12:1306. https://doi.org/10.3390/ma12081306